Numerical Study on the Design of Reinforced Soil by Vertical Micropiles

A. Kamura[1], J. Kim[2], T. Kawai[2], M. Kazama[2], N. Hikita[3] and S. Konishi[3]

[1]*Department of Civil Engineering, National Institute of Technology Fukushima College, Fukushima, Japan*

[2]*Department of Civil and Environmental Engineering, Graduate School of Engineering, Tohoku University, Sendai, Japan*

[3]*Geo-technical Division, Hirose Co., Ltd., Osaka, Japan*

[1]*E-mail*: kamura@fukushima-nct.ac.jp

ABSTRACT: The mechanical behavior of the reinforced soil by vertically arranged micropiles was considered using the three-dimensional finite element analysis. To make effective use of space around the slope, soil needs to be reinforced using micropiles placed in a small area. The main objective of this investigation was to evaluate the mechanical influence of various micropile arrangements and to determine the effects of pile spacing for design purposes. Numerical simulations of three cases using different pile angles indicated the amount of slope displacement and the values of the sectional force of the micropiles differed significantly. Among the three cases, the maximum slope displacement was 1.7 times the minimum value. Finally, numerical simulations of three cases using different pile spacing was carried out to clarify the effects of pile spacing on the amount of slope displacement and the sectional force of the micropiles.

KEYWORDS: Reinforced soil, Vertical micropiles, Finite element analysis, Parametric study

1. INTRODUCTION

In slope stabilization work, a reinforced soil method with ground anchors or piles is generally adopted. The most common method involves placing the piles perpendicular to the inclined slope surface. However, this method has a serious limitation: the front of the slope area becomes unusable during the construction period. As a consequence, social and financial losses are experienced in countries like Japan with limited land availability. A new method of reinforcing slopes that does not render so much land unusable is clearly required.

Soil reinforcement using micropiles is prevalent around the world. The common purpose of this method is to under-pin the soil, e.g. Stocker et.al (1979), Miki et.al (1985) and Jaydip et.al (2015). Another common practice involves using micropiles as a preventive against landslides, e.g. Esmaeili, M. (2013), Sun, S.W. et.al (2013) and John, P.T. et.al (2013). As the use of micropiles is becoming increasingly common, design manuals are being drawn up around the world to ensure the application is carried out properly, e.g. US Department of Transportation (DOT) (2005).

A serious drawback of this method of slope stabilization is that it is difficult to evaluate the micropile behavior because the micropiles are narrower than typical piles and have lower stiffness. While some landslide prevention works have utilized micropiles, it is rare that micropiles are placed vertically near the tip of the slip line on sloped ground. While integral behavior is expected to some extent at least in the soil surrounding the micropiles, the relatively sparse placement of micropiles near the tip of slip line on the slope makes it difficult to evaluate the behavior of the surrounding soil. While there are precedents of micropiles use for slope reinforcement in Japan, the reinforcement mechanism has yet to be elucidated. Moreover, since micropiles are low in stiffness, the method is accompanied by some ground deformation. As such, it is necessary to evaluate the influence of the pile deformation mode on the amount of deformation. Both the pile spacing and pile angle are known to contribute to the deformation mode.

The authors aim to establishing a reliable design method of reinforced soil by vertically arranged micropiles. This method involves utilizing a narrow flat space at the middle height of a slope to access the surrounding area (see Figure 1). To clarify the reinforcement mechanisms of micropiles and the behavior of surrounding soils, a three-dimensional finite element (FE) analysis was performed in this investigation. The analysis was carried out with the virtual slope model to evaluate the influence of the pile arranged patterns. The analysis involved the simulation of a staged construction with steep excavation, and the evaluation of the mechanical behavior of the slope reinforced by vertically arranged micropiles (see Figure 2).

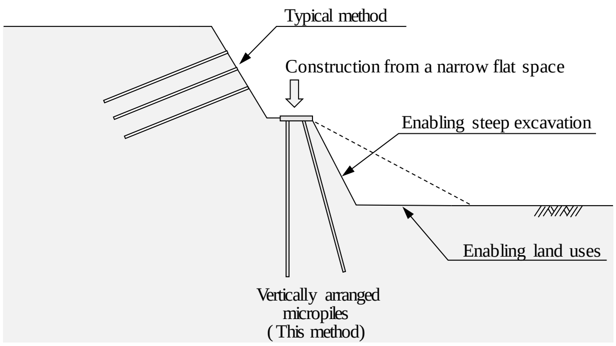

Figure 1 Overview of reinforced soil method by vertically arranged micropiles

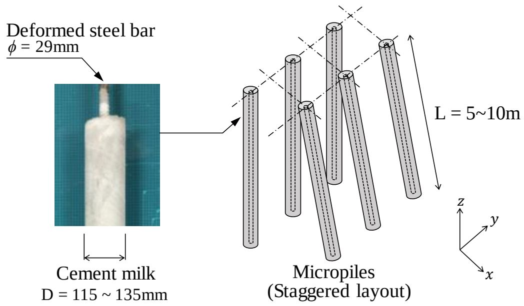

Figure 2 Overview of micropiles

The FE code PLAXIS 3D is used for all analysis discussed here. The design parameters, including the pile angle and the pile spacing, are the focus of this study. The relationship between the pile angle and the slip line of the slope was considered for three patterns of pile arrangement. Similarly, the influence on the cross-sectional force and the slope deformation of the micropile spacing was evaluated. To complete the FE analysis and clarify the effects of pile spacing, pile spacing was varied between 0.4 to 0.6 m (with 0.1m increments in the y-axis direction of Figure 2.).

In addition to this, the amount of deformation and cross-sectional force of the pile was evaluated in relation to the deformation modes of the reinforced soil. Focusing on the deformation mode makes it possible to take the earth pressure, which is an external force, into account in establishing a practical design method for reinforcing soil by vertically arranged micropiles.

2. MODELING AND CONSTITUTIVE LAWS

2.1 Modeling overview

The mechanical behavior of slope stabilization works with soil reinforced by vertically arranged micropiles is simulated with the use of the three-dimensional FE code PLAXIS 3D. The primary reason for adopting the 3D FE analysis is to evaluate such design parameters as the pile angle and spacing.

In this paper, the virtual slope model is designed to simulate the reinforcement mechanisms of the micropiles as well as the soil behavior. The 3D numerical model used in this study, with L=50m and W=5.5m and a pile spacing of 0.4 to 0.6m (in 0.1m increments) in the y-axis direction, is shown in Figure 3. The outer diameter of the micropile is 115mm and it consists of cement milk with a design strength of 24N/mm^2 and deformed steel bar with a diameter of 29 mm. This model consists of two slopes, H=4m, and the gradient of each slope was set to 1:1.5 at the initial condition of the analysis. Then the behavior of the soil mass due to its own weight and to the staged steep excavation of the slope (gradient 1:0.5) after the placing of the micropiles was simulated by a static elasto-plastic analysis in the drained condition.

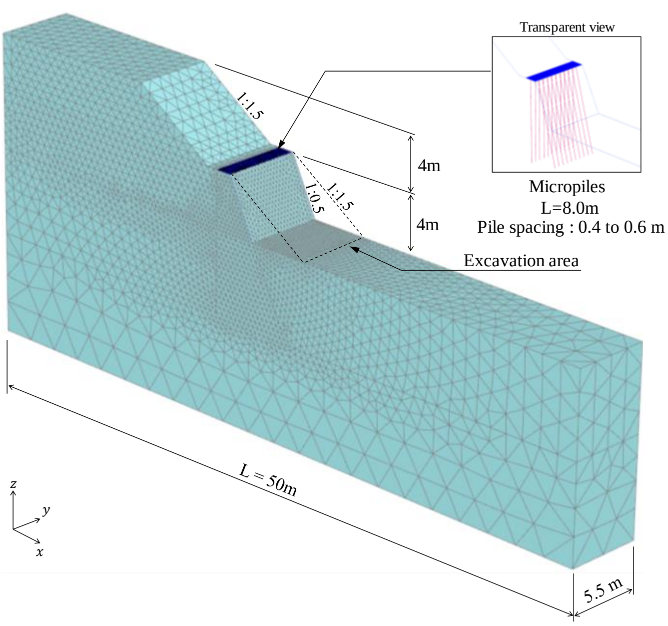

Figure 3 3D numerical model

2.2 Soil model

The soil layer was modelled in the PLAXIS 3D with the Hardening Soil Model (HS model), which is based on the Mohr-Coulomb failure criterion. The strain region considered was smaller than the strain-softening phase since the reinforced method of this type cannot be applied on soft ground composed of cohesive soil. Therefore, the HS model, which considers only hardening behavior, was adopted in this paper. A basic feature of the HS model is the stress dependency of soil stiffness. The loose condition due to the staged excavation for slope reinforcement by micropiles can be expressed using this model.

The underlying principle of the formulation of the HS model is the hyperbolic relationship between deviatoric stress and vertical strain. This model is derived from the hyperbolic model developed by Duncan and Chang (1970), with some improvement on the hyperbolic formulation for elasto-plastic model (Schanz et al., 1999). This hyperbolic function for the standard drained triaxial test can be described as

$$-\varepsilon_1 = \frac{1}{E_i}\frac{q}{\left(1-q/q_a\right)} \quad , \quad \text{For}: \ q < q_f \tag{1}$$

$$E_i = \frac{2E_{50}}{2-R_f} \tag{2}$$

where ε_1 is the axial strain, R_f is the failure ratio, q is the deviatoric stress, and q_a is the asymptotic value of the shear strength. These relationships are plotted in Figure 4 as the result of standard drained triaxial test. The ultimate deviatoric stress q_f and the quantity of q_a are defined as

$$q_f = (c\cot\phi - \sigma'_3)\frac{2\sin\phi}{1-\sin\phi} \tag{3}$$

$$q_a = \frac{q_f}{R_f} \tag{4}$$

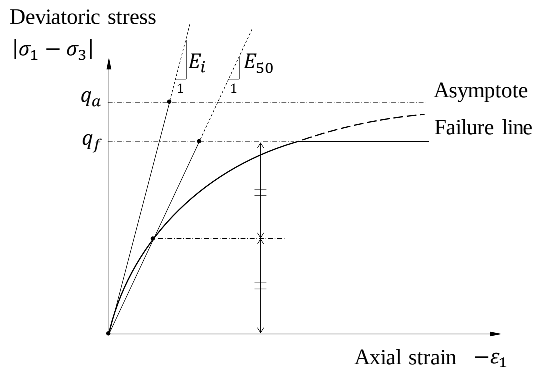

Figure 4 Hyperbolic stress–strain relationship for a standard drained triaxial test (Schanz et al.,1999)

This relationship is derived from the Mohr-Coulomb failure criterion, which involves the parameters c and ϕ. The parameter E_{50} is the confining stress dependent stiffness modulus for primary loading and is given as

$$E_{50} = E_{50}^{\text{ref}}\left(\frac{c\cos\phi - \sigma'_3\sin\phi}{c\cos\phi + p^{\text{ref}}\sin\phi}\right)^m \tag{5}$$

where E_{50}^{ref} is a reference stiffness modulus corresponding to the reference stress p^{ref}, and m is the power of stress dependency. Soos von (2001) reported a range of m values from 0.5 to 1 depending on soil types. The input parameters used in this model are shown in Table 1. In addition, the shear hardening yield function and the cap yield function, defined by Schanz et al. (1999), were adopted in this study. The shear yield function is defined as

$$f_s = \frac{2}{E_i}\frac{q}{(1-q/q_a)} - \frac{2q}{E_{\text{ur}}} - \gamma^{\text{p}} \tag{6}$$

$$\gamma^{\text{p}} = -\left(2\varepsilon_1^{\text{p}} - \varepsilon_{\text{v}}^{\text{p}}\right) \approx -2\varepsilon_1^{\text{p}} \tag{7}$$

where γ^{p} is the hardening parameter, $\varepsilon_{\text{v}}^{\text{p}}$ is plastic volumetric strain and ε_1^{p} is plastic strain component in triaxial condition. The cap-type yield surface is integrated to close the elastic region. The cap yield surface is defined as

$$f_c = \frac{\tilde{q}^2}{M^2} + p'^2 - p_{\mathrm{p}}^2 \tag{8}$$

with $p' = \dfrac{\sigma'_1 + \sigma'_2 + \sigma'_3}{3}$

$$\tilde{q} = \sigma'_1 + (\alpha - 1)\sigma'_2 - \alpha\sigma'_3\,, \qquad \alpha = \frac{3 + \sin\phi}{3 - \sin\phi}$$

where M is a material parameter which relates to K_0-value, p_p is an isotropic pre-consolidation stress. Both the shear locus and the yield cap are hexagonally shaped due to the Mohr-Coulomb failure criterion. The analysis was performed on the drainage conditions in all cases since the focus in this investigation is on the long-term mechanical behavior.

Table 1 Soil parameters of HS model

Parameter	Value	Unit
E_{50}^{ref}	7.0×10^3	kN/m^2
p^{ref}	100.0	kN/m^2
c	5.0	kN/m^2
ϕ	30.0	°
ψ	1.0	°
ν	0.33	-
γ_{unsat}	18.0	kN/m^3
R_f	0.9	-
m	0.5	-

2.3 Structural model

Since the diameter of the micropile is small compared to the pile length, the micropile is modelled as an embedded beam element model of Sadek and Shahrour (2004). This structural model consists of beam elements with embedded interface elements to describe the interaction with the soil at the pile skin and the pile foot (Figure 5). It has been pointed out that the pile-ground interaction problem requires a three-dimensional FE analysis and an embedded beam element (e.g. F., Tschuchnigg et.al.(2013)). The beam element is set to linear elastic because the cement milk constituting the micropile exhibits almost linear behaviour until the actual point of failure, and the deformed steel bar (Diameter 29mm) in the core also behaves linearly for such strain. The capping concrete of micropiles is modelled as an elastic plate element.

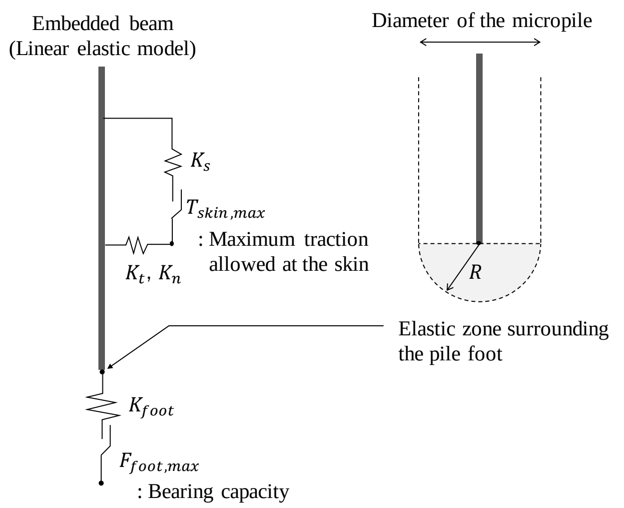

Figure 5 Embedded beam model in PLAXIS 3D

Tables 2 and 3 show the parameters of the embedded beam and the capping concrete in this study. The parameters of the beam element are set as with equivalent cross-sectional characteristics according to the ratio of the elastic modulus of the cement milk and the deformed steel bar. The interaction of the micropile with the soil at the pile skin is described by linear elastic behaviour with a finite strength T_{max}. This parameter, which was determined from the design provision for a ground anchor in this study, provides the maximum traction allowed at the skin of the embedded beam.

Table 2 Parameters of embedded beam

Parameter	Value	Unit
E	1.20×10^7	kN/m^2
γ	21.0	kN/m^3
A	2.05×10^{-2}	m^2
I	9.1×10^{-6}	m^4
$T_{skin,max}$	36.1	kN/m
$F_{foot,max}$	15.6	kN

Table 3 Parameters of capping concrete

Parameter	Value	Unit
E	2.50×10^7	kN/m^2
G	1.04×10^7	kN/m^2
ν	0.2	-
γ	24.5	kN/m^3
t	0.3	m

3. ANALYSIS AND EVALUATION

3.1 Description of the case study

The three-dimensional finite element (FE) model adopted in the case study is presented in Figure 3. The FE mesh used approximately 132 thousand 10-node tetrahedral elements to represent the soil layers. All studies are carried out under the drained condition. The staged construction processes were expressed by the following phases:

1. Generation of initial stress condition
2. Activation of the micropiles and the capping concrete (embedded beam element and plate element)
3. First step excavation (gradient 1:0.5) in the slope of the lower section (2m: half the height of the slope)
4. Second step excavation (gradient 1:0.5) in the slope of the lower section (excavation of total 4m)

The analytical parameters of the case study are the pile angle and the pile spacing. As is shown in Figure 6, there are three possibilities taken into account for the placement of the micropiles. In addition to these variations in patterns, the impact of changing the spacing of the piles from 0.4m to 0.6m (with 0.1m increments in the y-axis direction of Figure 2) was also considered. Pile spacing in the x-axis direction at the pile head was as follows: Case 1 and Case 2 were fixed with 0.6m, and Case 3 was fixed with 1.1m. The pile spacing was determined conventionally in the design of this method. It should be noted that among the three cases with different pile angles, the results of structural stability using a current simplified design code were the

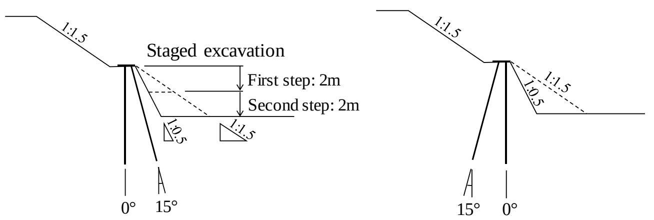

(a) Case 1 (b) Case 2

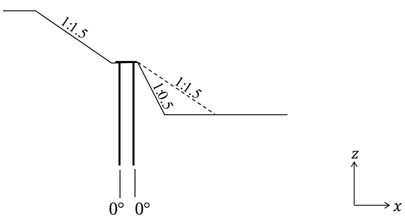

(c) Case 3

Figure 6 The pile arrangements for the case study

same. Therefore, the relationship between the deformation condition of the slope and each parameter on the design of this method is evaluated in this section.

3.2 Effects of pile angle

Figure 7. a-c shows the displacement distribution of the slope after excavation (gradient 1:0.5) in the center of the cross section for each case. A clear difference is confirmed in the displacement of the slope despite using the same specifications and the same spacing (the y-axis direction: 0.5m) of the micropiles. A potential slip line appeared through the toe of the slope in all cases. The maximum displacement of 15mm for Case 1 was the smallest among the case studies, and large deformations were noted for both Case 2 and Case 3. The maximum displacement was 25mm and 22mm for Cases 2 and 3, respectively. These values are in the range of 1.5-1.7 times larger than the displacement in Case 1. Besides the particularly large amount of slope displacement in Case 2, a large amount of deformation was also noted at the top of the first slope. Furthermore, as can be seen from Figures 7b and 7c, the displacement distribution for Cases 2 and 3 indicates a tendency to deform up to the top of the second slope with the slip line. The deformation at the toe of slope is rebound due to the release of stress. In practice, however, this should not pose a problem since the area of influence is limited to the excavation area, whereas the amount of rebound is considerably larger.

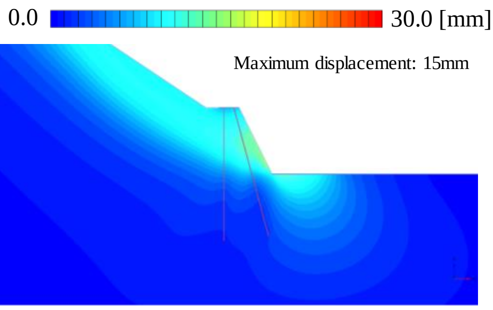

(a) Case 1

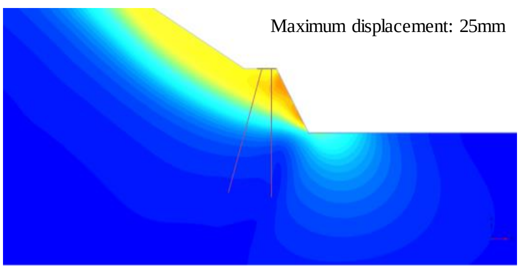

(b) Case 2

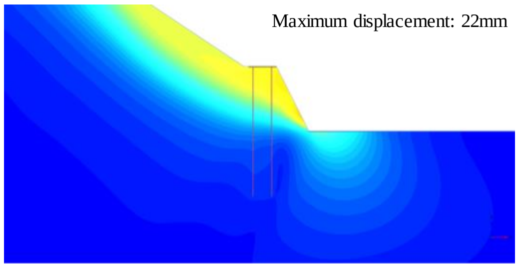

(c) Case 3

Figure 7 Total displacement distribution of the slope in the center of the cross section after excavation

In terms of safety, the global safety factor of Case 1 is Fs = 1.36, and Case 2 and Case 3 are Fs =1.20 and Fs =1.23, respectively. That is, there were differences between the cases even in terms of their global safety factor. A smaller amount of deformation results in a higher safety factor. The safety analysis was calculated by the strength reduction method proposed by Brinkgreve and Bakker (1991). The global safety factor was obtained by reducing the strength parameter of the standard Mohr-Coulomb model. Since the HS model used in this study is based on the Mohr-Coulomb model, the analysis result of HS model was used as the initial condition of the safety analysis.

From these results, it can be determined that the three cases, which have equal stability according to the currently used simplified design code, are not equal in terms of the expected slope deformation. Figure 8 shows the distribution of settlement. When evaluating the influence of slope excavation on the surrounding area, the estimation of vertical displacement is important. The amount of displacement and the area of influence of both Cases 2 and 3 are greater than Case 1. Therefore, if it is necessary to reduce the vertical displacement at the top of the slope, it would be advised to choose Case1. However, if it is not possible to apply Case1 due to construction conditions, Case 2 or Case 3 can be adopted.

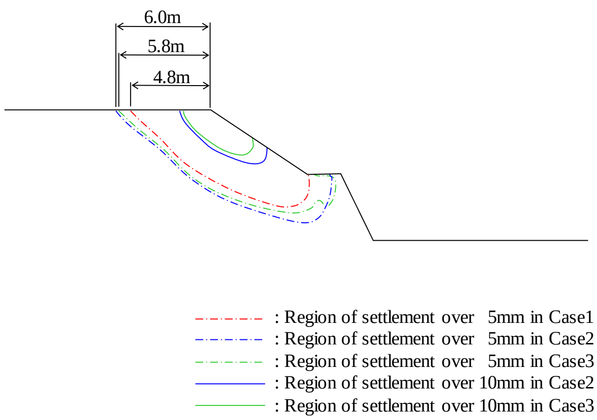

Figure 8 Distributions of settlement over 5mm and 10mm

The mode of micropile deformation, with a 50 fold magnification, is shown in Figure 9. All cases behave like a cantilever beam supported at a leg by a reaction force spring without any significant settlement. However, the amount of displacement at the pile head and the deformation mode differ for each case. In Case 1, the deformation mode involves the micropiles expanding at the center at the middle height of the slope, whereas in Cases 2 and 3 a large amount of deformation occurs at the pile head. Moreover, the deformation mode of Case 2 occurs in a state in which the pile head is largely rotated, while in Case 3, the pile head moves horizontally.

For such low stiffness piles, both Cases 2 and 3 must be considered undesirable states. The deformation modes of Cases 2 and 3 are caused by significant cross-sectional force in the micropiles governed by the ground deformation. Clearly, the layout of the micropiles is important in terms of providing sufficient reinforcement to suppress deformation.

Figure 10 shows the relationship between the direction of the maximum principal stress and the angle of the micropile. When using thin piles which fall within the allowed range of the pile strength or pile surface friction, the deformation of the slope will be restrained with a more equal direction of maximum principal stress and angle of the pile (See Figure 9a). In contrast, the amount of deformation will increase when using low rigidity piles as a bending reinforcement (Figure 9b). The method typically involves reinforcing the ground rationally by the micropiles by placing them in the same direction of the maximum principal stress. From this point of view, this reinforce method is selected when there are restrictions on the construction area, despite not being the "best solution" in terms of rational mechanics.

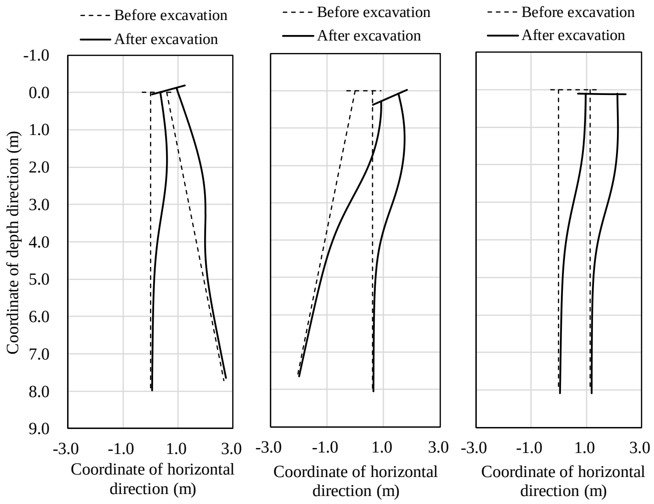

(a) Case 1 (b) Case 2 (c) Case 3

Figure 9 Deformation mode of the micropiles after slope excavation with a step gradient of 1:0.5 (magnification 50x)

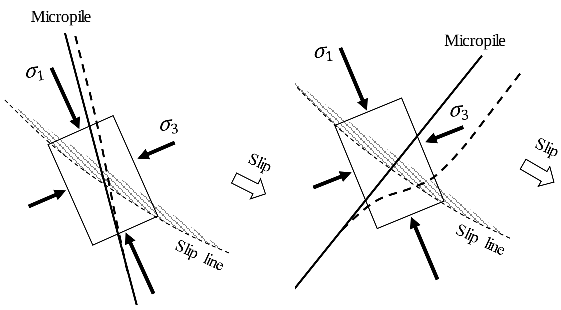

(a) Compressional reinforcement (b) Bending reinforcement

Figure 10 Relationship between the direction of the maximum principal stress and angle of the micropile

The differences in the three cases becomes clearer when the cross-sectional forces in the micropiles is considered. The axial forces in the micropiles after the excavation (gradient 1:1.5 to 1:0.5) are plotted in Figures 11a-c. The micropiles in each case behave as friction piles since the axial forces is close to zero at the pile foot despite the bearing capacity of the piles, as shown in Table 2. However, these results indicate that the mechanical roles of the micropiles differ. This can be attributed to the different directions of the maximum principal stress and the different angles of the micropile. Accordingly, it was found that the micropiles at the front side and rear side exhibit different behavior even in the same case. It should be noted that the value of allowable compressive force for micropiles is 130 kN, and that the value of allowable bending moment is 1.5kNm. The material parameters relating to these values were reported by Ohtani et.al (2004). (Note that buckling was not taken into consideration in the study cited).

The axial force in Case 1 is well-balanced from the perspective of the value and distribution of the force. This is attributed to the better conditions in mechanical rationality previously mentioned (Figure 11.a). By contrast, in Case 2, the axial force in the micropile at the rear is smaller than that in other cases (Figure 11.b). Since only the micropiles at the front bear the earth pressure, deformation progresses. Because this reinforcement method uses piles with low rigidity, a high level of mechanical efficiency is required. The axial force in Case 3 is well-balanced from the perspective of the distribution of the force, much like Case 1 (Figure 11c). However, the slope experiences considerable deformation despite the large value of axial force, as can be seen in Figure 7c.

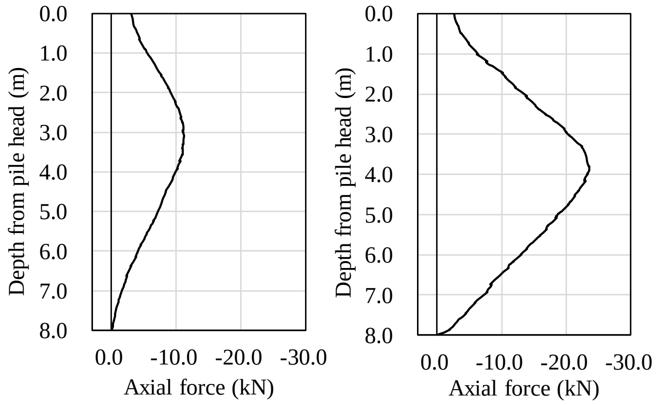

The rear The front

(a) Resulting axial forces in the micropiles of Case 1

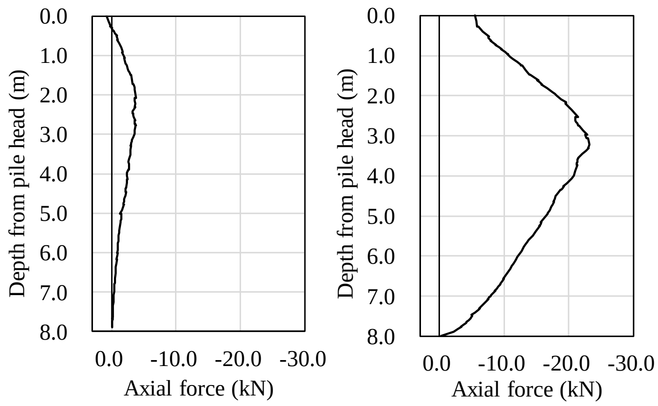

The rear The front

(b) Resulting axial forces in the micropiles of Case 2

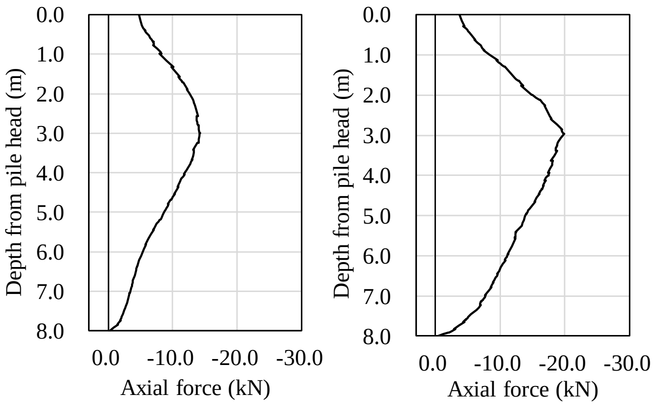

(c) Resulting axial forces in the micropiles of Case 3

Figure 11 Resulting axial forces in the micropiles

A comparison of all three cases reveals that the pile layout in Case 1 is the most rational reinforcement pattern for the practical application of this reinforcement method. These results indicate that the angle of at least one column of micropiles should ideally coincide with the direction of the maximum principal stress in order to reduce deformation.

Another consideration in determining the optimum pile configuration for such use of micropiles in slope stabilization is buckling. The risk of buckling increases due to the axial force exerted by the surrounding ground on the micropiles, which have rather low stiffness. Moreover, when a bending moment is exerted on a thin pile, the buckling strength is significantly reduced. Furthermore, in order to bear a large axial force, the prerequisite is sufficient adherence between the micropile and the surrounding ground. In addition to the requirement for "direct" adherence, it is important that the area close to the surface of the micropiles is not characterized by significant plasticity. This is because the force is not transmitted efficiently unless the state of soil around the micro pile is elastic. This is not an issue that can be ignored and is a particularly important consideration in seismic design. The impact of soil plasticity and elasticity in seismic design and slope evaluation are longstanding problems to be addressed in further studies.

The bending moments in the micropiles are shown in Figure 12. In all three cases, the bending moment approaches zero at the pile foot. At the pile head, however, the tendencies in the bending moment differ considerably. The bending moment at the rear side in Case 2 is the largest among all of the cases, as shown in Figure 12.b. The large amount of slope deformation in Case 2 can be explained in that the bending moment approaches the maximum allowable value.

In order to reduce the bending moment in the micropiles, one possible approach is to reduce the spacing between the piles to reduce the burden on each pile. (It should be noted that the diameter of micropiles is fixed due to the limitation of the casing machine.) Moreover, it has been shown that the likelihood of soil loosening (due to the movement of soil mass or erosion) between the micropiles increases when the piles are placed in a sparse configuration, e.g. Zhang, M. et.al (2004) and Nishigata, T. et.al (2005). Therefore, from an engineering point of view, close spacing is clearly desirable. However, an increase in the number of piles means that construction costs also become higher. It is therefore important to establish the most appropriate spacing between the piles considering both the geotechnical engineering perspective and the cost of construction.

The friction force of the surface of the micropiles in Case 1 is shown in Figure 13. Clearly, the micropiles at the front are more effective than those at the rear in terms of mechanical rationality. Moreover, since the distribution of the friction force switches sign (positive and negative) in the near boundary of ground level, it can be assumed that just under the ground level the reaction force is such that it creates a friction pile. One of the prerequisites for this method is that the micropiles are capable of bearing such friction force. From this perspective, evaluating the interaction between the peripheral ground and the micropiles in terms of friction force is important in the design of this method. Therefore, since the friction force of the micropile surface varies depending on the specific conditions, each parameter affecting each of the micropiles needs to be considered in more detail in future work. In addition, the cause of the irregularities in the results for friction force is presumed to be the effect of the mesh. In practice, the actual diameter of the micropiles is considerably smaller than the size of the mesh. This has led the irregular trend which appears in the results for friction force using this FE mesh.

3.3 Effects of pile spacing

The relationship between the spacing of micropiles and the normalized maximum amount of the slope displacement in Case 1 is shown in Figure 14. The FE analysis was carried out by changing the pile spacing in the y-axis direction from 0.4 to 0.6 m (in 0.1m increments). The results indicate that the amount of slope deformation increases as the space between the piles increases. The nonlinear characteristics of effects of the pile spacing weakly appear. The results indicate that the pile group effect appears clearly when the load is larger than that applied in this study or when the amount of deformation is greater than that in this study. Field experience suggests that the ideal pile spacing for this method was estimated as between 2 and 7 times the diameter of the pile. The quantitative evaluation of the relationship between pile spacing and deformation is a topic for a more in depth analysis in the future.

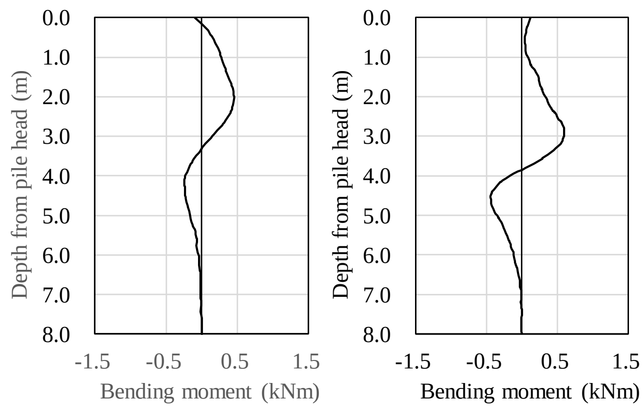

(a) Resulting bending moments in the micropiles of Case 1

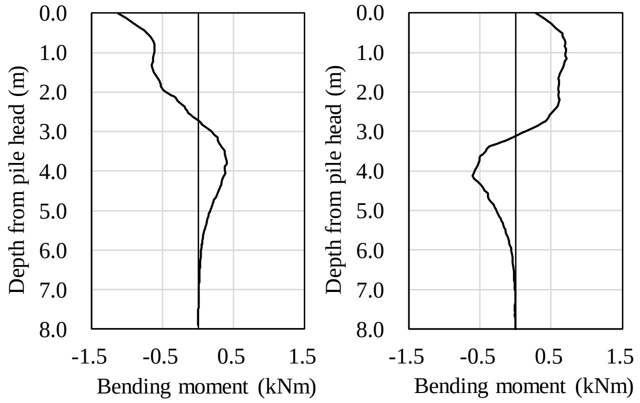

The rear The front

(b) Resulting bending moments in the micropiles of Case 2

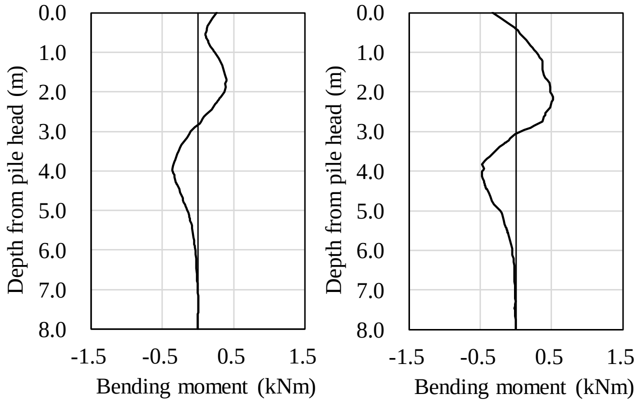

The rear The front

(c) Resulting bending moments in the micropiles of Case 3

Figure 12. Resulting bending moments in the micropiles

The axial force and the bending moment in the micropiles on each pile spacing is shown in Figure 15. While the values do increase with increased space between the piles, the trend of the axial force is actually more pronounced than the bending moment. The sensitivity of the pile spacing to the bending moment is not high, since the micropiles at the front behave mainly as "compressional reinforcement" piles in Case 1. In addition to this, the horizontal earth pressure tends to be transferred from micropile to micropile even as slope deformation progresses, and this trend is exacerbated with increased spacing between the micropiles. This is a point which cannot be neglected when deciding the design standards for such low stiffness piles with such a small diameter.

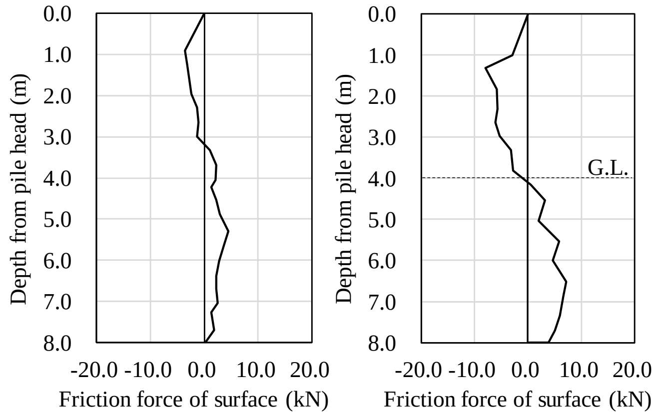

The rear The front

Figure 13 Friction force distribution of the micropile surface in Case 1

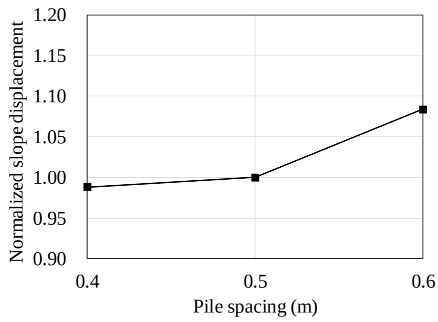

Figure 14 Relationship between the micropile spacing and the maximum amount of the slope displacement in Case 1

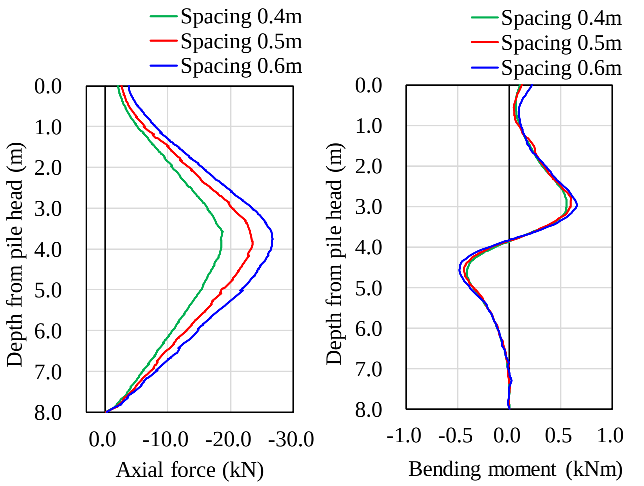

Figure 15 Axial forces and bending moments in the front micropiles for each pile spacing in Case 1

In future, the mechanical behavior of micropiles spaced more widely apart must be examined. Erosion between the micropiles is also an issue which must also be taken into consideration with regard to pile spacing. Optimal design conditions can be established by determining the maximum allowable cross-sectional force or slope deformation. In order for the design of this method to be improved from the current simple design code, a complex set of evaluations need to be carried out to determine both the mechanical behavior of the piles and to predict the amount of deformation.

3.4 Modeling of the external force on the design

To establish a rational design method for reinforced soil by vertically arranged micropiles, it is necessary to model the external force. The distribution of the deviatoric strain in Case 1 is shown in Figure 16. This confirms that the potential slip line runs through the back portion of the micropiles. It is also clear that the potential slip line extends toward the top of the slope at a fixed angle (Kamura et.al 2016).

The Coulomb earth pressure theory is commonly employed when establishing the external force in the design of retaining walls. Also in the method described in this paper, it is desirable that the external force is modeled by a simple set of values based on the Coulomb theory for practical design. In such a method, it is probable that the region surrounding the micropiles is set to a virtual wall, which is modelled like a soft reinforced concrete structure, and the Coulomb earth pressure acts as the external force. The shape of the earth pressure used to calculate the resultant force is determined by the distribution shape of the deviatoric strain.

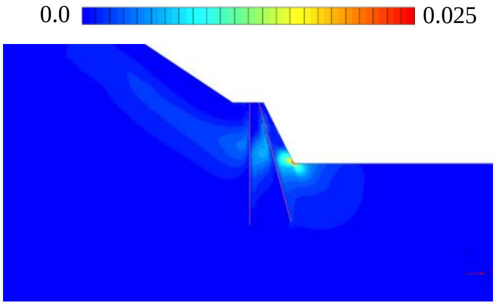

Figure 16 Distribution of the deviatoric strain in Case 1

In this study, an FE analysis was carried out with the forced displacement applied to the region surrounding the micropiles as a virtual wall (assuming a rigid body) to make it easier to consider the distribution of the deviatoric strain. The distribution of the deviatoric strain due to a forced displacement of 0.2m is shown in Figure 17. The similarity in the tendency of the deviatoric strain in Figures 16 and 17 is similar indicates good agreement between the results given by calculating the angle of the slip line using the FE analysis and determining the slip line using the Coulomb theory. The resultant

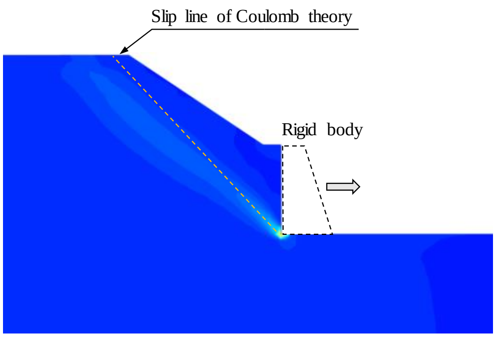

Figure 17 Distribution of the deviatoric strain by applying a forced displacement of 0.2m

forces for the active earth pressure agreed well with each other at 43kN and 40kN using the FE analysis and Coulomb theory, respectively.

The resultant forces of the active earth pressure obtained by the FE analysis of Case 1, the FE analysis applied to the forced displacement, and the Coulomb theory are shown in Figure 18. The values of the resultant force approached the value given by the Coulomb theory with increased displacement. It should be noted that the error values of FE analytical solution were larger as displacement increases, because the formulation of the soil model in this paper assumes a small amount of deformation. The results obtained by the FE analysis of Case 1 are approximately double those obtained using the Coulomb theory. For the ground composed of strain-hardening soil, the results show the possibility of modeling the external force using a function based on the Coulomb theory. However, to do this effectively the pile spacing must not cause any loosening of the soil between the micropiles.

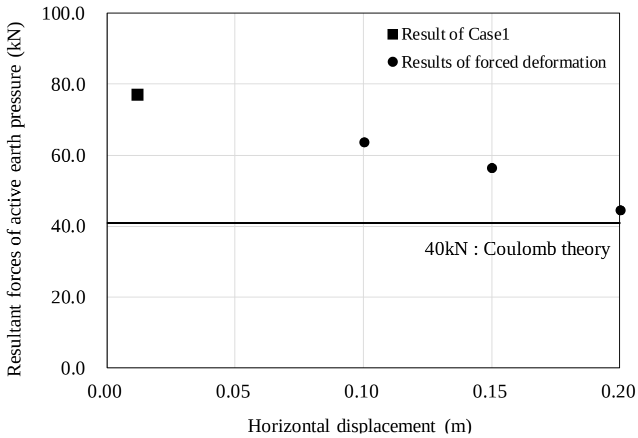

Figure 18 The resultant forces of the active earth pressure for each result (FE analysis of Case 1, FE analysis which applying the forced displacement, and Coulomb theory)

The distributions of the horizontal earth pressure at the rear of the micropiles in Case 1 and the case of forced deformation 0.1m are shown in Figure 19. The triangular shape of the distribution is consistent with that of horizontal earth pressure. On the other hand, the distribution shape of the forced deformation of 0.1m is not triangular: rather, the value near the top becomes larger. The shape of this distribution pattern shares the same tendency as that reported by Fang, Y. et. al (1994). However, in order to verify the internal stability of the practical design, using a triangular distribution is appropriate since the design target is the region of small deformation (an approximately elastic region) in practical design. In addition, it is necessary to combine the earth pressure, as the external force of the design, with the vertical earth pressure since the vertically arranged micropiles bear the vertical component of the earth pressure. In a future project, the authors are considering modeling the external force (the design force) of the design to match the deformation mode shown in Figure 9 by combining the earth pressure between the vertical component and the horizontal component.

Once the relationships mentioned above are quantitatively clarified, it will be possible to apply them to a practical design. Ideally, the value obtained by the Coulomb theory will be used as the external force for the virtual wall (the region surrounded by the micropiles) in the verification of external stability. Additionally, the value of the external force estimated by a function which springs from this idea will be used to verify the internal stability of the virtual wall. To this end, it is necessary to clarify the relationships and the functions to model the external force for the design in future research.

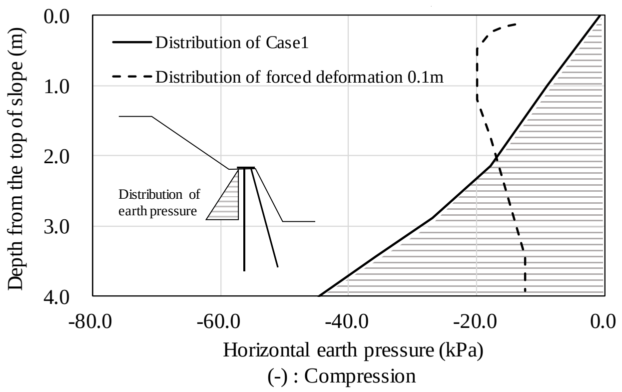

Figure 19 The distribution of the horizontal earth pressure at the rear of the micropiles in Case 1

4. CONCLUSION

This paper provides an overview of a numerical study on the design of reinforced soil by vertically arranged micropiles using a three-dimensional FE analysis. Simulations were performed to clarify the reinforcement mechanisms of micropiles considered together with soil behavior. The focus of this study was on such design parameters as the pile angle and pile spacing.

The stabilities of the three cases (Cases 1-3) have the same value according to the current simplified design code even though the angle of the piles in each case is different. In an evaluation of the slope deformation of these three cases, it was shown that the three cases are by no means equal. In addition, it is necessary to ensure that the pile angle is similar to the direction of maximum principal stress in order to restrain the deformation of the slope.

The maximum amount of the slope deformation and the cross-sectional force in the micropiles increases with increasing space between the piles. In Case 1 it was shown that the influence of the axial force at the front is more pronounced than the bending moment since the micropiles of front behave mainly as "compressional reinforcement" piles.

In order to model the external force for the practical design, the distribution of deviatoric strain was described. The potential slip line extends toward the top of the slope at a fixed angle in Case 1. The trend of the shape of the slip line was similar to the FE analysis applied to the forced displacement and the Coulomb theory. The results show the possibility of modeling the external force based on the Coulomb theory in the design for ground composed of strain-hardening soil.

As an issue for practical design, the design criteria are required for the following: cases that can be designed with simple modeling and cases that should be designed in detail by finite element analysis. The authors plan to clarify exactly which parameters are required for the computer aided design for this construction method in future research.

5. REFERENCES

Brinkgreve, R.B.J., and Bakker, H.L. (1991). Non-linear finite element analysis of safety factors, Proceedings of the 7th International Conference on Computational Methods and Advances in Geomechanics, 1117–1122.

Duncan, J.M., Chang, C.Y. (1970). Nonlinear Analysis of Stress and Strain in Soils. Journal of Soil Mechanics and Foundation Division, ASCE 96(5), 1629–1653.

Esmaeili, M., Gharouni, M. and Khayyer, F. (2013). Static and Dynamic Analyses of Micropiles to Reinforce the High Railway Embankments on Loose Beds, Journal of Rehabilitation in Civil Engineering 1-2, 39-48.

Fang, Y., Chen, T., and Wu, B. (1994). Passive Earth Pressures with Various Wall Movements. J. Geotech. Engrg., ASCE, 1307-1323.

F., Tschuchnigg and H.F., Schweiger (2013). Comparison of Deep Foundation Systems using 3D Finite Element Analysis Employing Different Modeling Techniques, Geotechnical Engineering Journal of SEAGS & AGSSEA, Vol.44, No.3 September.

Jaydip, V. C., Jayeshkumar, P., J. J., Bhavsar. (2015). Micro-Pile: Recent advances and future trends, International Conference on: "Engineering: Issues, opportunities and Challenges for Development, S.N. Patel Institute of Technology & Research Centre, Umrakh, Bardoli

John, P.T., and Martin, H. (2013). Design Method for Slide-Stabilizing Micropile Walls, Geo-Congress 2013, ASCE,1971-1983

Kamura, A., Kim, J., Kawai, T., Kazama, M., Hikita, N. and Konishi, S. (2016). Numerical simulation on the installation pitch of compressional reinforced soil method as retaining wall for existing embankment, 51st. Japan national conference on geotechnical engineering, 1549-1550 (in Japanese).

Miki, G., Sakashita, I., and Kodama, H. (1983). Practical examples of the reticulated root pile method in Japan, Soil mechanics and foundation engineering, No.1398, 35-40 (in Japanese).

Nishigata, T., Nishida, K. and Inaba, S. (2005). Mechanism of Reinforcement and Restraint Effect of Soil Nailing Method in Cut Slope, Journal of the Society of Materials Science, Japan, Vol.54, No.11, 1153-1158.

Ohtani, Y., Sakamoto, R., and Yoshioka, A. (2004). Field Measurement of Abutment Foundation by Reinforced Soil for Natural Ground, 39st. Japan national conference on geotechnical engineering, 1509-1510 (in Japanese).

Plaxis B.V. (2013). Plaxis 3D manual 2013, Delft, Netherlands.

Sadek, M., Shahrour, I. (2004). A three dimensional embedded beam element for reinforced geomaterials, International Journal for Numerical and Analytical Methods in Geomechanics, 28, 931-946.

Schanz, T., Vermeer, P.A., Bonnier, P.G. (1999). The Hardening Soil Model: Formulation and Verification, Beyond 2000 in Computational Geotechnics. Balkema, Rotterdam, 281-296.

Soos von, P. (2001). Properties of Soil and Rock (in German), Grundbau-taschenbuch, vol.1, 6th Ed., Ernst and Son, Berlin, 117–201.

Stocker, K.F., Korber, G.W., Gassler, G. and Gudehus, G. (1979). Soil nailing, C.R. Coll. Int Reinforcement des Soils, Paris.

Sun, S.W., Zhu, B.Z., Wang, J.C. (2013). Design method for stabilization of earth slopes with micropiles, Soils and Foundations, 53(4), 487–497.

US Department of Transportation (2005). Micropile Design and Construction Guidelines, Implementation Manual.

Zhang, M., Sensho, K., et.al. (2004). Experiment and application of the high-tensile wire mesh to slope stabilization, 39st. Japan national conference on geotechnical engineering, 2133-2134 (in Japanese).